Genomic characterization of three novel Desulfobacterota classes expand the metabolic and phylogenetic diversity of the Phylum

Chelsea L. Murphy[1], James Biggerstaff[1], Alexis Eichhorn[1], Essences Ewing[1], Ryan Shahan[1], Diana Soriano[1], Sydney Stewart[2], Kaitlynn VanMol[1], Ross Walker[1], Payton Walters[1], Mostafa S. Elshahed[1], and Noha H. Youssef[1]*

[1]Department of Microbiology and Molecular Genetics, Oklahoma State University, Stillwater, OK, USA

[2]Department of Animal Sciences, Oklahoma State University, Stillwater, OK, USA

Running Title: Three novel classes in the Desulfobacterota

*: Corresponding author: Mailing address: Oklahoma State University, Department of Microbiology and Molecular Genetics, 1110 S Innovation Way, Stillwater, OK 74074. Phone: (405) 744-1192, Fax: (405) 744-1112. Email: noha@okstate.edu.

Abstract. An overwhelming majority of bacterial life remains uncharacterized. Recent efforts to assemble genomes from metagenomes have provided invaluable insights into these yet-uncultured bacterial lineages. We report on the characterization of 30 genomes belonging to three novel classes within the phylum Desulfobacterota. One class (proposed name *Candidatus* "Anaeroferrophillalia") was characterized by the capacity for heterotrophic growth, either fermentatively or utilizing polysulfide, tetrathionate and thiosulfate as electron acceptors. Autotrophic growth using the Wood Ljungdahl pathway and hydrogen or Fe(II) as an electron donor could also occur in absence of organic carbon sources. The second class (proposed name *Candidatus* "Anaeropigmentia") was characterized by its capacity for fermentative or aerobic growth at low oxygen thresholds using a broad range of sugars and amino acids, and the capacity to synthesize the methyl/alkyl carrier CoM, an ability that is prevalent in the archaeal but rare in the bacterial domain. Pigmentation is inferred from the capacity for carotenoids (lycopene) production, as well as the occurrence of the majority of genes involved in bacteriochlorophyll *a* biosynthesis. The third class (proposed name *Candidatus* "Zymogenia") was characterized by the capacity for heterotrophic growth fermentatively using broad sugars and amino acids as carbon sources, and the adaptation of some of its members to hypersaline habitats. Analysis of the distribution pattern of all three classes showed their occurrence as rare community members in multiple habitats, with preferences for anaerobic terrestrial (e.g. hydrocarbon contaminated environments, wetlands, bioreactors), freshwater (e.g. ground water and gas-saturated temperate lakes), and marine (e.g. hydrothermal vents, marine sediments, and coastal sediments) environments, over oxygenated (e.g. pelagic ocean and agricultural land) settings. Special preference for some members of the class *Candidatus* "Zymogenia" to hypersaline environments, e.g. hypersaline microbial mats and lagoons was observed.

68 **Importance.** Culture-independent diversity surveys conducted in the last three decades have
69 clearly demonstrated that the scope of microbial diversity is much broader than that inferred
70 from isolation efforts. Multiple reasons have been put forth to explain the refractiveness of a
71 wide range of the earth's microbiome to isolation efforts. Documenting the scope of high-rank
72 phylogenetic diversity on earth, as well as deciphering and documenting the metabolic
73 capacities, physiological preferences, and putative ecological roles of these yet-uncultured
74 lineages represents one of the central goals in current microbial ecology research. Recent efforts
75 to assemble genomes from metagenomes have provided invaluable insights into these yet-
76 uncultured lineages. This study expands our knowledge of the phylum Desulfobacterota through
77 the characterization of 30 genomes belonging to three novel classes. The analyzed genomes were
78 either recovered from Zodletone Spring in southwestern Oklahoma in this study, or recently
79 binned from public metagenomes as part of the Global Earth Microbiome initiative. Our results
80 expand the high-rank diversity within the bacterial tree of life by describing three novel classes
81 within the phylum Desulfobacterota, document the utilization of multiple metabolic processes,
82 e.g. iron-oxidation, aromatic hydrocarbon degradation, reduction of sulfur-cycling intermediates,
83 and features, e.g. coenzyme M biosynthesis, and pigmentation, as salient characteristics in these
84 novel Desulfobacterota classes.

Introduction

Traditional approaches to characterize bacterial and archaeal taxa have long hinged upon isolation procedures. Despite decades of such efforts, much of the microbial world remains uncultured. Culture-independent surveys utilizing the 16S rRNA gene as a phylogenetic marker have long been utilized to characterize yet-uncultured microbial diversity. However, while useful for documenting the identity, relative abundance, and distribution patterns of microorganisms, such surveys provide limited information on community interactions, metabolic inferences, or microbial growth rates (1-3). The development and wide-scale utilization of genome-resolved metagenomics and single cell genomic approaches have yielded a wealth of metagenome-assembled genome (MAGs) and single-cell amplified genome (SAGs) assemblies (3, 4). In addition to successfully recovering representative genomes of uncultured lineages previously defined by 16S rRNA gene surveys (4), such efforts have also expanded the bacterial tree of life by recovering representatives of novel lineages that previously eluded detection even by culture-independent diversity surveys (5, 6).

Further, the accumulation of MAGs and SAGs has also been leveraged for enacting phylogenomic-based taxonomic schemes that encompass both cultured and uncultured microorganisms (7). The genome taxonomy database (GTDB) utilizes 120 bacterial single-copy genes, average nucleotide identity (ANI), alignment fractionation, and specific quality controls to provide a detailed (phylum to species) genome-based taxonomy (8). The current release (r95) encompasses 111 phyla, 327 classes, 917 orders, 2,282 families, 8,778 genera, and 30,238 species. While broadly agreeing with organismal and 16S rRNA gene-based outlines, e.g. (9), the GTDB proposes several name and rank changes. For example, the Gram-positive Firmicutes are proposed to constitute seven different phyla (Firmicutes A-G). Within the Proteobacteria, the

class Betaproteobacteria was reclassified as an order within the class Gammaproteobacteria, and the Epsilonproteobacteria was elevated to a new phylum (Campylobacterota) (7).

Perhaps nowhere was the effect of genomics-based taxonomy more profound than in the class Deltaproteobacteria. The Deltaproteobacteria encompassed anaerobic respiratory and fermentative/syntrophic lineages, the Myxobacteria, *Bdellovibrio*-like predators, and aquatic oligotrophs. The disparate physiological preferences, metabolic capacities, and lifestyles within the Deltaproteobacteria have long been noted, and prior efforts based on single and concatenated gene phylogenies have reported its polyphyletic nature (10). The recent genome-based taxonomy in GTDB r95 has proposed splitting this group into 16 phyla, including 4 distinct cultured phyla: Desulfobacterota, Myxococcota, Bdellovibrionota, and SAR324 (11).

The recently enacted phylum Desulfobacterota encompasses sulfate-reducing and related fermentative and syntrophic lineages previously constituting the bulk of strict anaerobes within the Deltaproteobacteria. GTDB r95 lists 20 classes, 31 orders, 119 families, and 279 genera, of which 12, 14, 38, and 86, respectively, contain cultured representatives. Cultured members of the Desulfobacterota have been identified in a plethora of marine, freshwater, terrestrial, and engineered ecosystems exhibiting wide ranges of salinities, pH, and temperatures (12). Cultured Desulfobacterota show preference to anoxic conditions, and many utilize sulfate, sulfite, thiosulfate, elemental sulfur, or iron (or combinations thereof) as the terminal electron acceptor in respiratory and/or disproportionation processes (13-16). In addition, some grow fermentatively or in syntrophic partnerships (17, 18).

During a broad effort to characterize the yet-uncultured diversity within Zodletone spring, a sulfide and sulfur-rich spring in southwestern Oklahoma, using genome-resolved metagenomics, we recovered multiple MAGs that appear to represent distinct novel classes

131 within the phylum Desulfobacterota. In addition, a recent global effort for binning genomes from
132 publicly available metagenomic datasets (19) yielded additional MAGs belonging to these novel
133 Desulfobacterota classes. Here, we report on the genomic characteristics of 30 MAGs that appear
134 to collectively represent three novel additional classes within the Desulfobacterota. In addition to
135 providing a detailed characterization of their metabolic capacities, physiological preferences, and
136 structural features, we also document their global ecological distribution.

Materials and Methods

Sample collection, DNA extraction, and metagenomic sequencing.

Samples were collected from the source sediments of Zodletone Spring, located in western Oklahoma's Anadarko Basin (N34.99562° W98.68895°). The geochemistry of the spring has previously been described (20-23). Samples were obtained from the anoxic sulfidic black sediments at the source of the spring using sterile spatulas and were deposited into sterile 50 mL polypropylene plastic tubes. The samples were transferred to the laboratory on ice and immediately processed. DNA extraction was performed using the DNeasy PowerSoil kit (Qiagen, Valencia, CA, USA) according to manufacturer protocols. The extracted DNA was sequenced using the services of a commercial provider (Novogene, Beijing, China) using the Illumina HiSeq 2500 platform. 281.0 Gbp of raw data were obtained. Contigs were assembled using MegaHit (24), and binned using both Metabat (25) and MaxBin2 (26). DasTool was used to select the highest quality bins from each metagenome assembly (27). Bins that showed contamination levels >5% and/or strain heterogeneity of >10% were further refined and cleaned based on taxonomic affiliations of the bins, GC content, tetranucleotide frequency, and coverage levels using RefineM (28). Bins were classified using the classification workflow option - classify_wf of GTDB-Tk (8) (v 1.3.0), and 5 bins belonging to novel Desulfobacterota classes were selected for further analysis. In addition, we identified genomes belonging to the Desulfobacterota within the recently released 52,515 genomes in the earth microbiome catalogue collection (19) that were deposited in IMG/M database**.** Of these, 25 genomes belonging to novel Desulfobacterota classes were downloaded from the IMG/M database (May 2020) and included in the analysis.

Genomes quality assessment and general genomic features.

Genome completeness, genome contamination, strain heterogeneity, and GC content were assessed using CheckM (v 1.0.13) (29). Genomes with >50% completion and <10% contamination (n=30) were used for further analysis (Tables S1, S2). Selected MAGs were designated as medium or high-quality drafts based on the criteria set forth by MIMAGs (30). The 5S, 16S, and 23S rRNA sequences were identified using RNAmmer (v 1.2) (31). tRNA sequences were identified and enumerated with tRNAscan-SE (v 2.0.6, May 2020) using the -G general tRNA model (32).

Phylogenomic analysis.

Preliminary classification was carried out using GTDB-Tk (8) with the -classify_wf option. Further phylogenomic analysis was conducted using the 120 single-copy marker genes concatenated alignment that was generated by GTDB-Tk (7). A maximum-likelihood phylogenetic tree was constructed in RAxML (v 8.2.8) (33) with the PROTGAMMABLOSUM62 model and default settings, using members of the phylum Bdellovibrionota as an outgroup. Tree phylogeny, along with average amino acid identity (AAI), calculated using the AAI calculator [http://enve-omics.ce.gatech.edu/]), were used to determine putative taxonomic ranks. The arbitrary AAI cutoffs used were 49%, 52%, 56%, and 68% for class, order, family, and genus, respectively.

Functional annotation.

Protein-coding genes were annotated using Prodigal (v 2.50) (34). Identified protein-coding genes were assigned KEGG orthologies (KO) using BlastKOALA (35), and metabolic pathways were visualized with KEGG mapper (36). For more targeted analysis of functions of interest, hidden markov model (HMM) profile scans were performed on individual genomes. All genomes were queried with custom-built HMM profiles for sulfur metabolism, electron transport

chain complexes, and chlorophyll biosynthesis. Custom profiles were built from Uniprot reference sequences for all genes with an assigned KO number, which were downloaded, aligned with Clustal-omega (37), and assembled into a profile with the hmmbuild function of HMMer (v 3.1b2) (38). For genes without a designated KO number, a representative protein was queried against the KEGG genes database using Blastp, and hits with e-values $<1e^{-80}$ were downloaded, aligned, and used to construct an HMM profile as described above. HMM scans were carried out using the hmmscan function of HMMer (38). A thresholding option of -T 100 was used to limit results to alignments with a score of at least 100 to improve specificity. Further confirmation was achieved through phylogenetic assessment and tree building procedures. Briefly, putatively identified sequences were aligned with Clustal-omega (37) against the reference sequences used to build the HMM database and placed into a maximum-likelihood phylogenetic tree using FastTree (v 2.1.10) (39). Sequences that clustered with reference sequences were deemed to be true hits and were assigned a corresponding KO number. FeGenie (40) was used to predict the presence of iron reduction and iron oxidation genes in individual bins. Hydrogenases were identified using HMM scans with profiles constructed from alignments from the Hydrogenase Database (HydDB) (41) using a cutoff e-value of $1e^{-20}$.

Search for photosynthetic reaction center.

Identification of genes involved in chlorophyll biosynthesis in class "Anaeropigmentia" genomes prompted us to search the genomes for photosynthetic reaction center genes. HMM profiles for Reaction Center Type 1 (RC1; PsaAB), Reaction Center Type 2 (RC2; PufLM and $PsbD_1D_2$) (pfam00223 and pfam00124, respectively), PscABCD (Chlorobia-specific; custom built), PshA/B (Heliobacteria-specific; custom built) (42), as well as the newly identified Psa-like genes from Chloroflexota (43) were used to search the genomes for potential hits using hmmscan. A

structurally-informed reaction center alignment (42, 44) was additionally used. The best potential hits were modeled using the SWISS-MODEL homology modeler (45) to check for veracity.

Ecological distribution

A near-complete 16S rRNA gene from each class was selected as a representative for querying against 16S rRNA databases. Representative sequences were queried against two different databases: 1. The IMG/M 16S rRNA publicly available assembled metagenomes (46), where an e-value threshold of $1e^{-10}$, percentage similarity ≥90%, and either ≥80% subject length for full-length query sequences or ≥80% query length for non-full-length query sequences criterion were applied, and 2. The GenBank nucleotide (nt) database (accessed November 2020), using a minimum identity threshold of 90%, ≥80% subject length alignment for near full-length query sequences or ≥80% query length for non-full-length query sequences, and a minimum alignment length of 100 bp. Hits meeting the selection criteria were then aligned with 16S rRNA reference gene sequences from each class using Clustal-Omega (37), and the alignment was used to construct maximum-likelihood phylogenetic trees with FastTree (39). The environmental source of hits clustering with the appropriate reference sequences were then classified with a scheme based on the GOLD ecosystem classification scheme (47). Phylogenetic trees were visualized and annotated in iTol (48).

Sequence and MAG accessions

Metagenomic raw reads for Zodletone sediment are available under SRA accession SRX9813571. Zodletone whole genome shotgun project was submitted to GenBank under Bioproject ID PRJNA690107 and Biosample ID SAMN17269717. The individual assembled MAGs have been deposited at DDBJ/ENA/GenBank under the accession JAFGAM000000000, JAFGAS000000000, JAFGFE000000000, JAFGIX000000000, JAFGSY000000000. The

229 version described in this paper is version JAFGAM010000000, JAFGAS010000000,

230 JAFGFE010000000, JAFGIX010000000, JAFGSY010000000.

Results

Three novel classes within the Desulfobacterota.

Thirty Desulfobacterota MAGs binned from Zodletone spring sediments and 12 different locations (Table 1, Table S1) clustered into three distinct clades comprising 7, 17, and 6 genomes, that were unaffiliated with any of the 20 currently recognized Desulfobacterota classes in GTDB r95 taxonomic outline (Table 1, Table S1, Figure 1). Average amino acid identity (AAI) and shared gene content (SGC) values between these genomes and representative genomes from all other classes within the Desulfobacterota ranged between 41.63% ± 0.96% – 42.71% ± 1.04% (AAI), and 44.52% ± 4.28% – 51.61% ± 4.37% (SGC), confirming their distinct suggested position as novel classes within the Desulfobacterota phylum (Table S1). Further, the obtained Relative Evolutionary Divergence (RED) values of 0.38 – 0.42 confirmed the distinct class-level designation for all three lineages (Table S1). 16S rRNA gene sequences extracted from representative genomes placed all three groups as members of the "uncultured Deltaproteobacteria" bin within the class Deltaproteobacteria, Phylum Proteobacteria using the RDP-II taxonomic outline (Table S1). In SILVA taxonomic outline release 138.1 (9), these clades were classified as unclassified members of the order Desulfobacterales (clade 1), members of the phylum Sva085 (clade 2), and as uncultured members of the Desulfobacterota phylum (clade 3) (Table S1). We hence propose accommodating these 30 genomes into three distinct classes, for which the following names are proposed based on defining metabolic characteristics predicted from their genomes as described below: *Candidatus* "Anaeroferrophillalia" (order Anaeroferrophillales, family Anaeroferrophillacea), with the MAG assembly 3300022547 (*Anaeroferrophillus wilburensis*) serving as the type material. The name reflects its preference for anaerobic environments and observed capacity to utilize Fe(II) as a

supplementary electron donor in absence of organic substrates. *Candidatus* "Anaeropigmentia" (order Anaeropigmentiales, family Anaeropigmentiaceae), with the MAG assembly 3300022855_4 (*Anaeropigmentus antarcticus*) serving as the type material. The name reflects its preference for anaerobic environments and predicted capacity for pigment biosynthesis. *Candidatus* "Zymogenia" (order Zymogeniales, family Zymogeniaceaea), with the MAG assembly Zgenome_24 (*Zymogenus saltonus*) serving as the type material (GenBank assembly accession number JAFGIX000000000). The name reflects its preference for a fermentative mode of metabolism (zymo: Greek for digestion and fermentation). The representative type material MAG was chosen based on the MAG quality deduced from the % completeness (>90%), % contamination (<5%), and the presence of a rRNA operon in the assembly (Table S2). Below, we provide a more detailed analysis of the metabolic capacities, physiological preferences, and ecological distribution of each of these three classes.

Structural, physiological, and metabolic features

Class "Anaeroferrophillalia".

General genomic features: Genomes belonging to Class "Anaeroferrophillalia" possess average sized genomes (2.80 ± 0.33 Mbp), GC content (52.66% ± 5.63%), and gene length (937.07 ± 37.07 bp) (Table 1). Structurally, members are predicted to have a Gram-negative cell wall based on the possession of lipopolysaccharide (LPS) biosynthesis-encoding genes, and lack of genes encoding the pentaglycine linkage of peptidoglycan. The presence of the rod-shape determining genes *rodA*/*mreB*, and the genes encoding flagellar assembly suggest rod-shaped flagellated cells. Defense mechanisms include CRISPR defense systems, and Type I restriction endonucleases (Table S3). No evidence for special intracellular structures, e.g. bacterial microcompartments, nanocompartments, or magnetosomes, were identified (Table S3).

Physiological features: Members of class "Anaeroferrophillalia" appear to be strict anaerobes, based on the absence of respiratory cytochrome C oxidase (complex IV) components, the presence of the oxygen-limited cytochrome bd complex, and the identification of the oxidative stress enzymes catalase, rubrerythrin, rubredoxin, alkylhydroperoxide reductase, and peroxidase (Table S3). Osmoadaptive capabilities are predicted via the identification of glycine betaine/proline ABC transporter ProXWV.

Heterotrophic fermentative capacities: Genomes of Class "Anaeroferrophillalia" possess robust biosynthetic capacities with few amino acids and cofactors auxotrophies (Table S3). The presence of genes encoding the EMP and the non-oxidative PPP pathway indicate heterotrophic growth capabilities. However, a limited number of sugars (glucose, fructose, mannose) appear to support growth (Figure 2A). As well, the capacity to degrade amino acids appears to be limited (Figure 2A, Table S3), and the lack of genes encoding the beta-oxidation pathway precludes potential growth on medium- and long-chain fatty acids. On the other hand, all genomes encode the lactate utilization enzyme D-lactate dehydrogenase (cytochrome) [EC:1.1.2.4], suggesting the capability to grow on D-lactate (Figure 2A). As well, the pathway for anaerobic benzoate metabolism appears to be present in all genomes, suggesting a specialty in degradation of aromatic compounds (Figure 2A). Pyruvate generated from D-lactate or sugar metabolism could be metabolized to acetyl-CoA via pyruvate ferredoxin oxidoreductase [EC: 1.2.7.1] encoded in all genomes, followed by conversion of acetyl-CoA to acetate with concomitant substrate level phosphorylation via the acetate CoA ligase [EC: 6.2.1.13] (Figure 2A, Table S3).

Respiratory capacities: In addition to fermentative capacities, possible respiratory activities were identified in class "Anaeroferrophillalia". Possible electron donors identified based on genomic analysis include D-lactate via the D-lactate dehydrogenase [EC: 1.1.2.5]. This enzyme has been

300 studied in several sulfate reducers and its physiological electron acceptor was found to be
301 ferricytochrome c3, which could serve as an entry point to an ETS, with the electrons possibly
302 moving to the genomically-encoded Qrc membrane complex (menaquinone reductase [EC:1.97.-
303 .-], onto the quinone pool and eventually to the terminal electron acceptor. Several hydrogenase-
304 encoding genes were identified in the genomes of class "Anaeroferrophillalia". These include the
305 periplasmic [Ni Fe] HyaABC (HydDB group 1d), predicted to be involved in hydrogenotrophic
306 respiration (as well as other hydrogenases that are predicted to be involved in recycling reduced
307 equivalents as explained below). Hydrogenotrophic respiration would proceed through the
308 periplasmic hydrogenase moving electrons from H_2 onto a periplasmic cytochrome C, the Qrc
309 membrane complex, the quinone pool, and eventually to the terminal electron acceptor.
310 Further, analysis of iron metabolism genes in members of class "Anaeroferrophillalia"
311 genomes indicated their possession of operonic DFE_0448-0451 and DFE_0461-0465 genes,
312 similar to the systems first identified in *Desulfovibrio ferrophilus* (Figure 2B) (49). In the
313 proposed *D. ferrophilus* model, electrons move from an external source, e.g. insoluble minerals
314 like iron, to an outer membrane cytochrome (encoded by DFE_0450 and DFE_0464 by each
315 respective system) through a complex of additional heme-containing periplasmic membrane-
316 bound (DFE_0449 and DFE_0461), periplasmic soluble (DFE_0448 and DFE_0462,
317 DFE_0465), or complex stabilizing (DFE_0451 and DFE_0463) cytochromes. Electrons could
318 potentially then pass on to menaquinone (49) and eventually to the terminal electron acceptor.
319 This later ETS is expected to operate possibly under substrate-limiting conditions (for example
320 in absence of D-lactate) as shown before for *D. ferrophilus* (49).
321 Possible electron acceptors identified include the sulfur cycle intermediates tetrathionate,
322 based on the identification of genes encoding the octaheme tetrathionate reductase (Otr) (50), as

well as the guanylyl molybdenum cofactor-containing tetrathionate reductase (TtrABC) (51). The produced thiosulfate from the action of either Otr or TtrABC could be metabolized through disproportionation, based on the identification of thiosulfate reductase *phsABC* genes (Figure 2B). Polysulfide reduction capability is also predicted based on the identification of genes encoding the membrane-bound molybdoenzyme complex PsrABC (52). No marker genes suggesting the ability to respire sulfate or sulfite were identified. Nitrate reduction genes were similarly lacking.

ATP production and recycling reduced equivalents: The genomes encoded complex I components; NADH dehydrogenase [EC: 7.1.12], as well as an F_1F_o-ATPase. With an incomplete oxidative phosphorylation pathway, we predict that the NADH dehydrogenase is possibly coupled to the quinone pool and cytochromes for generation of a proton motive force across the inner membrane that can then be used for ATP synthesis via the F_1F_o-ATPase, similar to the model predicted in the sulfate reducer *Desulfovibrio vulgaris* (53). Alternatively, or concomitantly, a proton-motive force could possibly be generated during the operation of Wood Ljungdahl (WL) pathway, encoded by all Class "Anaeroferrophillalia" genomes, in the homoacetogenic direction. In that case, a membrane-bound mechanism that achieves redox balance between heterotrophic substrate oxidation and the WL function as the electron sink (54, 55) is needed. Candidates for this membrane-bound electron bifurcation mechanism are the membrane-bound [Ni Fe] hydrogenase (Mbh) (HydDB group 4d), which couples reduced ferredoxin (produced via the action of pyruvate ferredoxin oxidoreductase [EC: 1.2.7.1]) oxidation to the reduction of protons to H_2, with the concomitant export of protons to the periplasm (54, 55). Recycling of electron carriers would further be achieved by the cytoplasmic

345 [NiFe]-hydrogenase (MvhAGD) plus the heterodisulfide reductase HdrABC, both of which
346 encoded in the genomes (HydDB group [Ni Fe] 3c) (Figure 2A).
347 *Autotrophic capacities:* In conditions where inorganic compounds, e.g. ferrous ions or H_2, serve
348 as electron donors, we expect autotrophic capacities to be fulfilled also via the WL pathway. In
349 that case, the proton gradient-driven phosphorylation (through the ATPase complex) will be the
350 only means for ATP production (56) as no net ATP gain by substrate level phosphorylation
351 (SLP) is achieved via the WL pathway (55). All genomes encode mechanisms for acetyl-CoA
352 (produced from WL pathway) conversion to pyruvate (Pyruvate:ferrodoxin oxidoreductase
353 [EC:1.2.7.1]), reversal of pyruvate kinase (including pyruvate-orthophosphate dikinase (EC
354 2.7.9.1), pyruvate-water dikinase [EC 2.7.9.2], as well as pyruvate carboxylase [EC:6.4.1.1] and
355 PEP carboxykinase (ATP) [EC:4.1.1.49]), and the bifunctional fructose-1,6-bisphosphate
356 aldolase/phosphatase to reverse phosphofructokinase.
357 ***Class* "Anaeropigmentia".**
358 *General genomic features:* Members of the Class "Anaeropigmentia" possess relatively large
359 genomes (3.96 ± 0.74 Mbp), with average GC content (47.29% ± 4.55%), and gene length
360 (912.46 ±44.91 bp) (Table 1). Cells are predicted to be Gram-negative rods, with CRISPR
361 systems, type I, and type III restriction endonucleases (Table S3).
362 *Physiological features:* Class "Anaeropigmentia" genomes encode two distinct pathways for the
363 biosynthesis of the compatible solute trehalose (both from ADP-glucose and glucose via
364 trehalose synthase [EC:2.4.1.245], as well as from UDP-glucose and glucose via the action of
365 trehalose 6-phosphate synthase [EC:2.4.1.15 2.4.1.347] and trehalose 6-phosphate phosphatase
366 [EC:3.1.3.12]), and its degradation via alpha,alpha-trehalose phosphorylase [EC:2.4.1.64]. The

367 genomes also encoded the capability for the storage molecule starch biosynthesis and
368 degradation.
369 *Heterotrophic capacities:* A heterotrophic lifestyle is predicted, based on the presence of a
370 complete EMP, and ED pathways, a complete TCA cycle, and both the oxidative and non-
371 oxidative branches of the PPP. Substrates predicted to support growth include sugars (glucose,
372 fructose, mannose, sorbitol), amino acids (alanine, aspartate, asparagine, glutamine, glutamate,
373 cysteine, serine), and fatty acids via the beta-oxidation pathway (Table S3, Figure 3A).
374 *Fermentative capacities:* The capability of class "Anaeropigmentia" to ferment pyruvate is
375 inferred by the presence of various pathways for end products (butanediol, acetate, ethanol, and
376 acetoin) generation (Table S3, Figure 3A).
377 *Respiratory capacities:* A complete electron transport chain with complexes I (NADH-quinone
378 oxidoreductase [EC: 7.1.1.2]), II (succinate dehydrogenase [EC: 1.3.5.1]), alternate complex III
379 (encoded by *actABCDEFG)*, and complex IV (cytochrome c oxidase cbb3-type
380 [EC: 7.1.1.9] as well as cytochrome bd ubiquinol oxidase [EC:7.1.1.7]), in addition to a V/A-
381 type as well as F-type H^+/Na^+-transporting ATPase [EC: 7.1.2.2], were identified suggesting
382 possible utilization of trace amounts of O_2 as a terminal electron acceptor by members of Class
383 "Anaeropigmentia". All Class "Anaeropigmentia" genomes encoded a complete Wood
384 Ljungdahl (WL) pathway. Additional ATP production via oxidative phosphorylation following
385 the generation of a proton-motive force during the operation of WL pathway, is therefore also
386 predicted. In that case, the RNF complex encoded in the majority of genomes would re-oxidize
387 reduced ferredoxin at the expense of NAD, with the concomitant export of protons to the
388 periplasm, thus achieving redox balance between heterotrophic substrate oxidation and the WL
389 function as the electron sink (54, 55). Recycling of electron carriers would further be achieved

by the cytoplasmic electron bifurcating mechanism (HydABC) plus MvhAGD-HdrABC, both of which are encoded in the genomes (HydDB groups [Fe Fe] A3, and [Ni Fe] 3c).

Specialized cofactor biosynthesis: Interestingly, the complete pathway encoding the phosphoenol pyruvate-dependent coenzyme M (CoM) biosynthesis was identified in all genomes of Class "Anaeropigmentia" (Figure 3A, Table S3). CoM is a hallmark of methanogenic Archaea, where it acts as a terminal methyl carrier that releases methane upon regeneration of its unmethylated state during methanogenesis (57). However, the utility of CoM in the bacterial domain is less understood. CoM was shown in the bacterial genera *Xanthobacter, Rhodococcus,* and *Mycobacterium* to be involved in propylene degradation as a carrier for a C3 carbon intermediate (58-60). Recently, the bacterial CoM biosynthetic cluster was identified in *X. autotrophicus* Py2 (61). The genes *xcbB1*, *C1*, *D1*, and *E1* encode the bacterial CoM biosynthetic operon, with only *xcbB1* showing homology to the archaeal CoM biosynthesis gene *comA* (61). The remainder of the genes *xcbC1*, *D1*, and *E1* are distinct from the archaeal genes *comBCDE*, and the bacterial biosynthetic pathway proceeds via a different route (61, 62). CoM biosynthesis genes identified in Class "Anaeropigmentia" genomes are distinct from the bacterial CoM biosynthesis genes *xcbC1*, *D1*, and *E1* and are indeed archaeal-like. Searching the functionally annotated bacterial tree of life AnnoTree (63) using the combination of KEGG orthologies corresponding to the archaeal CoM biosynthetic cluster *comABCDE* identified their collective presence in only 14 bacterial genomes from the phyla Acidobacteriota, Actinobacteriota, Bacteroidota, Chloroflexota, Desulfobacterota, Desulfobacterota_B, Latescibacterota, and Proteobacteria. Unfortunately, genes encoding additional enzymes required for propylene degradation (alkene monooxygenase, 2-hydroxypropyl-CoM lyase, 2-hydroxypropyl-CoM dehydrogenase, and 2-oxopropyl-CoM reductase) were absent in all class "Anaeropigmentia" genomes. Therefore,

additional research is required to confirm the expression of CoM biosynthesis genes, and further characterize its potential function, if any, in class "Anaeropigmentia".

Pigmentation: The majority of Class "Anaeropigmentia" genomes encode *crtB*, 15-cis-phytoene synthase [EC:2.5.1.32], and *crtI*, phytoene desaturase [EC:1.3.99.26 1.3.99.28 1.3.99.29 1.3.99.31], suggesting the capability of biosynthesis of lycopene from geranylgeranyl-PP. The gene encoding CrtY/L, lycopene beta-cyclase [EC:5.5.1.19], was however missing from all genomes, suggesting an acyclic carotenoid structure (Figure 3B). In addition to carotenoids, a large number of bacteriochlorophyll biosynthesis homologues were encoded in the majority of Class "Anaeropigmentia" genomes. These genes include *bchE* (anaerobic magnesium-protoporphyrin IX monomethyl ester cyclase), *bciB* (3,8-divinyl protochlorophyllide a 8-vinyl-reductase), and *chlLNB* (light-independent protochlorophyllide reductase subunits L, N, and B) catalyzing chlorophyllide a biosynthesis from Mg-protoporphoryin IX. In addition, a near complete pathway for the biosynthesis of bacteriochlolophyll *a* was encoded in the majority of Class "Anaeropigmentia" genomes. This includes the genes *bchXYZ* (3,8-divinyl chlorophyllide a/chlorophyllide a reductase subunits X, Y, and Z), *bchF* (3-vinyl bacteriochlorophyllide hydratase), *bchC* (bacteriochlorophyllide a dehydrogenase), and *chlP* (geranylgeranyl diphosphate/geranylgeranyl-bacteriochlorophyllide a reductase). However, *chlG* (chlorophyll/bacteriochlorophyll a synthase), which catalyzes the penultimate reaction of bacteriochlorophyllide *a* to geranylgeranyl-bacteriochlorophyllide *a*, was not identified (Figure 3B). Despite the presence of the majority of bacteriochlolophyll *a* biosynthetic genes in class "Anaeropigmentia", all attempts for the identification of a photosynthetic reaction center were unsuccessful.

Class "Zymogenia"

436 *General genomic features:* Genomes belonging to class "Zymogenia" possess average sized
437 genomes (3.7 ± 0.12 Mbp), GC content (54.4% ± 2.7%), and gene length (904.24 ± 62.85 bp)
438 (Table 1). Members of the class "Zymogenia" are Gram-negative rods with CRISPR and Type I
439 restriction endonucleases as defense mechanisms and no intracellular microcompartments (Table
440 S3).
441 *Physiological features:* Class "Zymogenia" genomes encode the capability for the compatible
442 solute trehalose biosynthesis both from ADP-glucose and glucose via trehalose synthase [EC:
443 2.4.1.245], as well as from UDP-glucose and glucose via the action of trehalose 6-phosphate
444 synthase [EC:2.4.1.15 2.4.1.347] and trehalose 6-phosphate phosphatase [EC:3.1.3.12]). No
445 genes encoding trehalose degradation were identified in Class "Zymogenia" genomes.
446 Biosynthesis and degradation of the storage molecule starch was encoded in the majority of
447 Class "Zymogenia" genomes. Multiple genes encoding oxidative stress enzymes (catalase,
448 rubrerythrin, rubredoxin, and alkylhydroperoxide reductase, peroxidase, and superoxide
449 reductase) were identified (Table S3).
450 *Heterotrophic fermentative capacities:* Class "Zymogenia" genomes encode a glycolytic
451 pathway, and a partial TCA pathway, suggesting heterotrophic capacities, possibly on a broad
452 repertoire of sugars including glucose, fructose, galactose, lyxose, arabinose, sorbitol, and xylitol
453 (Figure 4A, Table S3). Surprisingly, genes for fucose degradation to L-lactaldehyde (including
454 L-fucose/D-arabinose isomerase [EC:5.3.1.25, 5.3.1.3], L-fuculokinase [EC:2.7.1.51], and L-
455 fuculose-phosphate aldolase [EC:4.1.2.17]) were encoded in the majority of Class "Zymogenia"
456 genomes, but genes encoding the subsequent conversion of L-lactaldehyde to propanediol (L-
457 lactaldehyde reductase [EC:1.1.1.77]), as well as genes encoding propanediol utilization
458 (propanediol dehydratase [EC: 4.2.1.28]) were missing. Genomes did not encode genes

suggestive of aerobic (absence of complex III/ alternate complex III-encoding genes), or anaerobic respiratory capacities, but encoded pyruvate fermentation genes. These include formate C-acetyltransferase [EC: 2.3.1.54] and its activating enzyme [EC: 1.97.1.4] catalyzing pyruvate fermentation to formate and acetyl-CoA, pyruvate ferredoxin oxidoreductase [EC:1.2.7.11] catalyzing pyruvate oxidative decarboxylation to acetyl-CoA, followed by conversion of acetyl-CoA to acetate with concomitant substrate level phosphorylation via the acetate CoA ligase [EC: 6.2.1.13], and acetolactate synthase [EC: 2.2.1.6] and acetolactate decarboxylase [EC:4.1.1.5] for pyruvate conversion to (R)-Acetoin (Table S3, Figure 4A). The lack of a complete electron transport chain, or genes encoding for anaerobic respiratory processes, argue for a predominantly fermentative lifestyle.

ATP production and electron carrier recycling. Beside substrate level phosphorylation, ATP production is also possible via the PMF-utilizing H^+/Na^+-transporting ATPase [EC: 7.1.2.2] encoded in all genomes. All Class "Zymogenia" genomes encoded a complete Wood Ljungdahl (WL) pathway, and the majority encoded RNF complex. WL pathway in Class "Zymogenia" is predicted to function as an electron sink, and the membrane-bound RNF complex is predicted to help in the generation of a proton motive force across the inner membrane while re-oxidizing the reduced ferredoxin produced from the action of pyruvate ferredoxin oxidoreductase [EC:1.2.7.11]. The PMF generated could be used for ATP production via the complete the H^+/Na^+-transporting ATPase [EC: 7.1.2.2]. The cytoplasmic electron bifurcating mechanism (HydABC) plus the heterodisulfide reductase MvhAGD-HdrABC (also encoded in the majority of genomes) would function to recycle electron carriers in the cytoplasm (Figure 4A).

Ecological distribution

Class "Anaeroferrophillalia": Analysis of ecological distribution pattern identified 54, and 110 16S rRNA gene sequences affiliated with the class "Anaeroferrophillalia" in IMG (Figure 2C), and NCBI nt (Figure S1) databases, respectively (Nov-2020). While "Anaeroferrophillalia" genomes were recovered from a limited number of locations (marine sediments, hydrothermal vents, thermal spring, and Zodletone spring), 16S rRNA analysis expanded their ecological distribution to a range of terrestrial (primarily wetlands and hydrocarbon-impacted environments), marine (predominantly hydrothermal vents, but also coastal and marine sediments), and freshwater (temperate, ground and thermal springs) environments (Figures 2C, S1B-G). The observed distribution patterns reinforce the metabolically predicted preference of members of the "Anaeroferrophillalia" to hypoxic and anoxic settings, as evident by preferences to the oxygen-poor wetlands and hydrocarbon-impacted habitats over grassland and agricultural soils in terrestrial settings, and the preferences to vents and marine sediments over pelagic samples in marine settings. Nevertheless, given the low number of total sequence and the extremely low percentage relative abundance, it is clear that members of the class "Anaeroferrophillalia" are perpetual members of the rare biosphere, and are rarely successful to be a dominant community member in any ecosystem.

Class "Anaeropigmentia": Analysis of ecological distribution pattern identified 134 and 89 16S rRNA gene sequences affiliated with the class "Anaeropigmentia" in IMG (Figures 3C, S1B-G), and NCBI nt (Figure S1A) databases, respectively. While examined genomes were predominantly recovered from hypersaline environments (Ace Lake in Antarctica and Little Sippewissett salt marsh, MA, USA), the majority of 16S rRNA sequences associated with this group were largely associated with non-hypersaline freshwater temperate lake environments, e.g. Yellowstone Lake, the gas-saturated Lake Kivu, and a methane-emitting lake at the University of

Notre Dame. Terrestrial environments harboring members of class "Anaeropigmentia" were predominantly wetlands, with hydrocarbon-impacted habitats being the only other terrestrial setting. A limited presence in coastal marine setting and absence from marine pelagic environments was observed. Notably, many of the environments harboring members of class "Anaeropigmentia" are light-exposed, e.g. wetland surface sediment and lake water, justifying pigmentation, although many were not, e.g. coal mine soil and deep lake sediment. Similar to class "Anaeroferrophillalia", the limited number of affiliated 16S rRNA gene sequences suggests that members of class "Anaeropigmentia" are also part of the rare biosphere, present in small numbers across a range of different habitats.

Class "Zymogenia": Ecological distribution analysis identified only 44 and 33 16S rRNA gene sequences affiliated with the class "Zymogenia" in IMG (Figures 4B), and NCBI nt databases (Figure S1), respectively. A relatively high proportion of class "Zymogenia" 16S rRNA genes were recovered from oxygen-deficient environments, e.g. wetlands, marine sediments, and coastal sediments, as well as aquatic hypersaline settings, e.g. hypersaline lakes (Salton Sea) in California, and lagoons (Etoliko Lagoon in Greece). As well, a significant fraction of these sequences was recovered from anaerobic digestors and bioreactors environments, attesting to the preference of these organisms to anaerobic settings and adaptability of some its members to hypersaline environments (Figures 4B, S1B-G).

Discussion.

Genomic analysis for members of class "Anaeroferrophillalia" revealed the capability of heterotrophic growth on a limited number of substrates, either fermentatively or using sulfur-cycle intermediates (polysulfide, thiosulfate, and tetrathionate) as electron acceptors. Autotrophic growth using the WL pathway and utilization of H_2 or Fe(II) as electron donors for chemolithotrophic growth in absence of organic carbon sources could also be inferred. Analysis of ecological distribution patterns identified the occurrence of class "Anaeroferrophillalia" as a rare component in few, mostly anaerobic, habitats. Such limited distribution could be a reflection of the limited range of substrates supporting its growth, as well as its dependence on the sulfur-cycle intermediates thiosulfate and tetrathionate as electron acceptors, rather than the more abundant, stable, and ubiquitous sulfate. Although uncommon, microorganisms depending on specific sulfur intermediates (thiosulfate, S, sulfite, tetrathionate), but not sulfate, for growth have previously been reported (64, 65). Such pattern could be a reflection of metabolic interdependencies between various members of the sulfur cycle, a concept formulated based on the identification of a wide range of incomplete pathways in sequenced MAGs (5, 66). In addition, previous studies have shown that thiosulfate and other sulfur cycle intermediates (67, 68), as well as iron (69), were present in much higher levels, and played a more pronounced role in supporting microbial growth on earth during geological eons preceding the evolution of oxygenic photosynthesis. Oxygen production and accumulation from photosynthesis has led to the slow but inexorable oxidation of earth's surface (great oxidation event), and the establishment of sulfate as the predominant electron acceptor in the sulfur cycle (67). As such, rare lineages depending on H_2, Fe, and sulfur-intermediates (but not sulfate) for growth could represent lineages that thrived in a preoxygenated earth, but are rare nowadays.

Genomic analysis for members of Class "Anaeropigmentia" revealed a heterotrophic group of microorganisms capable of growing on sugars, amino acids, and fatty acids. Preference appears to be for anaerobic habitats, where it grows fermentatively, with predicted ability to grow under low oxygen microaerophilic conditions. Cells appear to be pigmented with carotenoids (Lycopene). While carotenoid pigments are known to be present in photosynthetic bacteria, where they increase the efficiency of photosynthesis by absorbing in the blue-green region then transferring the absorbed energy to the light-harvesting pigments (70), they also occur in a wide range of non-photosynthetic organisms, including Desulfobacterota, where they serve different purposes, including protection against desiccation (71), radiation (72), and oxidation (73). The occurrence of members of the class "Anaeropigmentia" in transiently and intermittently light-exposed habitats, e.g. lakes and wetlands, could justify their pigmentation, as well as their capability to detoxify trace amounts of oxygen via respiration. More intriguing is the presence of a near-complete machinery for bacteriochlorophyll *a* biosynthesis, a trait exclusive for photosynthetic organisms. However, despite the presence of these biosynthetic pathways, all our attempts for the identification of a photosynthetic reaction center (PRC) were unsuccessful. We argue that the failure to detect PRC-encoding genes in their genomes could be the result of either technical limitations, or the true absence of these genes. Technical limitations include, but are not limited to, contigs harboring PRC-encoding genes not binning from metagenomes; although this is highly unlikely when examining 17 genomes, many of which (n=9) have > 90% completion, and are binned from multiple metagenomic datasets using a variety of approaches. Another possibility for the failure of PRC genes identification could be the high sequence dissimilarity to known reaction center genes. Assuming true absence of PRCs, and hence photosynthetic capacities in class "Anaeropigmentia", how can the presence and

maintenance of most chlorophyll biosynthesis genes be justified? One possibility is the evolution of class "Anaeropigmentia" from a photosynthetic ancestor, with subsequent loss of PRC and some bacteriochlorophyll biosynthesis genes. Indeed, fragmented photosynthetic-related pathways have been previously discovered in multiple genomes, as we described recently (74). While the loss of the hugely beneficial photosynthetic capacity appears counterintuitive, even implausible, it could be explained in the context of a photosynthetic ancestor evolution to harvest thermal light in an ancient chemolithotrophic world, as previously proposed in (74, 75). These findings demonstrate that bacteriochlorophyll production alone should not be taken as a good measure of photosynthetic capability, and that fragmented pathways must be examined carefully when using bioinformatic tools to prevent any over-assumptions of function.

Finally, our genomic and ecological distribution pattern analysis for members of class "Zymogenia" predicted predominantly anaerobic fermentative organisms; and that some members of this novel class are adapted to growth under saline settings. We also note its extreme rarity in most examined settings. The underlying reason for such rarity is unclear, given its relatively wide substrate utilization range.

In conclusion, our work expands the metabolic and phylogenetic diversity of the Desulfobacterota through the description of 3 novel classes. Our analysis adds to the repertoire of ecological distribution and metabolic capabilities known for the phylum Desulfobacterota, with notable metabolic findings of iron metabolism, thiosulfate and tetrathionate reduction, near complete bacteriocholorophyll biosynthesis, carotenoid biosynthesis, CoM biosynthesis, and fermentation. Ecological distribution patterns observed reinforced and added context to the predicted metabolic capacities gleaned from genomic analysis. The study, overall, demonstrates

590 the utility of bioinformatic tools in exploring and defining unculturable organisms, helping to
591 bridge the vast knowledge gap presented by the uncultured majority.

592 **Acknowledgments**. This work has been supported by NSF grant 2016423 to NHY and MSE.
593 We thank the Hatzenpichler (Montana State University), Edwards (University of Toronto),
594 Bryant (Pennsylvania State University), Biddle (University of Delaware),and Cavicchioli (U of
595 New South Wales), laboratories for permitting access to metagenomes.

596 **Figure Legends.**

597 **Figure 1.** Maximum likelihood phylogenetic tree based on: (A) a concatenated alignment of 120
598 single-copy genes from all Desulfobacterota classes in GTDB r95, and (B) 16S rRNA gene for
599 Desulfobacterota classes with cultured representatives in GTDB r95. The three novel classes
600 described here are color-coded as shown in the legend. Bootstrap values (from 100 bootstraps)
601 are displayed for branches with ≥70% support. Members of the phylum Bdellovibrionota were
602 used as an outgroup (not shown).

603 **Figure 2.** Metabolic reconstruction and ecological distribution for members of the novel class
604 Candidatus "Anaeroferrophillalia". (A) Cellular metabolic reconstruction based on genomic
605 analysis of 7 genomes belonging to the novel class Candidatus "Anaeroferrophillalia". Substrates
606 predicted to support growth are shown in purple boxes, electron donors are shown in blue while
607 electron acceptors are shown in red. Fermentation end products are shown in pink. Sites of
608 substrate level phosphorylation are shown as red asterisks. All electron transport chain
609 components in the membrane are shown in green, while components for proton motive force
610 creation and electron carrier recycling are shown in orange. Grey dotted lines depict the
611 predicted flow of electrons from electron donors to electron acceptors. Green spheres in the
612 periplasmic space depict cytochromes. Abbreviations and gene names: EMP, Embden Meyerhoff
613 Paranas pathway; $Frd_{ox/red}$, Ferredoxin (oxidized/ reduced); Fru, fructose; Glu, glucose; Hdr,
614 heterodisulfide reductase complex; HyaABC, periplasmic [Ni Fe] hydrogenase; IM proteins,
615 inner membrane protein complex for the predicted iron oxidation system; LDH, L-lactate
616 dehydrogenase; Man, mannose; Mbh, membrane-bound [Ni Fe] hydrogenase; Mvh, Cytoplasmic
617 [Ni Fe] hydrogenase; OM proteins, outer membrane protein complex for the predicted iron
618 oxidation system; Otr, octaheme tetrathionate reductase; PhsABC, thiosulfate reductase;

619 PsrABC, polysulfide reductase; QrcABC, menaquinone reductase; Q pool, quinone pool;
620 RSH/RS-SR, reduced/oxidized disulfide; TCA, tricarboxylic acid cycle; TEA, terminal electron
621 acceptor; V, ATP synthase complex; WLP, Wood Ljungdahl pathway. (B) Phylogenetic
622 affiliation for Candidatus "Anaeroferrophillalia" thiosulfate reductase C subunit (PhsC, top) and
623 the iron oxidation complex protein DFE_0462 (bottom) in relation to reference sequences.
624 Candidatus "Anaeroferrophillalia" sequences are shown in red. Alignments were created in
625 Mafft (76) and maximum likelihood trees were constructed in RaxML (77). Bootstrap support
626 values are based on 100 replicates and are shown for nodes with >50% support. (C) Ecological
627 distribution of Candidatus "Anaeroferrophillalia"-affiliated 16S rRNA sequences. The middle
628 pie chart shows the breakdown of hit sequences based on the classification of the environments
629 from which they were obtained (classification is based on the GOLD ecosystem classification
630 scheme). Further sub-classifications for each environment are shown as smaller pie charts.
631 **Figure 3.** Metabolic reconstruction and ecological distribution for members of the novel class
632 Candidatus "Anaeropigmentia". (A) Cellular metabolic reconstruction based on genomic
633 analysis of 17 genomes belonging to the novel class Candidatus "Anaeropigmentia". Substrates
634 predicted to support growth are shown in purple boxes, electron donors are shown in blue while
635 electron acceptors are shown in red. Fermentation end products are shown in pink. Sites of
636 substrate level phosphorylation are shown as red asterisks. All electron transport chain
637 components in the membrane are shown in green, while components for proton motive force
638 creation and electron carrier recycling are shown in orange. Abbreviations and gene names:
639 CoM, coenzyme M; EMP, Embden Meyerhoff Paranas pathway; $Frd_{ox/red}$, Ferredoxin (oxidized/
640 reduced); fum, fumarate; Hdr, heterodisulfide reductase complex; HydABC, cytoplasmic [Fe Fe]
641 hydrogenase; I, II, aIII, and IV, aerobic respiratory chain comprising complexes I, II, alternate

642 complex III, and complex IV; Mvh, Cytoplasmic [Ni Fe] hydrogenase; PEP, phosphoenol
643 pyruvate; RNF, membrane-bound RNF complex; RSH/RS-SR, reduced/oxidized disulfide; succ,
644 succinate; TCA, tricarboxylic acid cycle; V, ATP synthase complex; WLP, Wood Ljungdahl
645 pathway. (B) Bacteriochlorophylls and carotenoid biosynthesis genes encountered in Candidatus
646 "Anaeropigmentia" genomes. Genes identified in at least one genome are shown in red boldface
647 text, while genes with no homologues in the genomes are shown in black text. MEP/DOXP, the
648 non-mevalonate DOXP/MEP (Deoxyxylulose 5-Phosphate/Methylerythritol 4-Phosphate)
649 pathway for isoprenoid unit biosynthesis. (C) Ecological distribution of Candidatus
650 "Anaeropigmentia"-affiliated 16S rRNA sequences. The middle pie chart shows the breakdown
651 of hit sequences based on the classification of the environments from which they were obtained
652 (classification is based on the GOLD ecosystem classification scheme). Further sub-
653 classifications for each environment are shown as smaller pie charts.
654 **Figure 4.** Metabolic reconstruction and ecological distribution for members of the novel class
655 Candidatus "Zymogenia". (A) Cellular metabolic reconstruction based on genomic analysis of 6
656 genomes belonging to the novel class Candidatus "Zymogenia". Substrates predicted to support
657 growth are shown in purple boxes, fermentation end products are shown in pink, and sites of
658 substrate level phosphorylation are shown as red asterisks. Components for proton motive force
659 creation and electron carrier recycling are shown in orange. Abbreviations and gene names: Ara,
660 arabinose; EMP, Embden Meyerhoff Paranas pathway; $Frd_{ox/red}$, Ferredoxin (oxidized/ reduced);
661 Fru, fructose; Gal, galactose; Glu, glucose; Hdr, heterodisulfide reductase complex; HydABC,
662 cytoplasmic [Fe Fe] hydrogenase; Lyx, lyxose; Mvh, Cytoplasmic [Ni Fe] hydrogenase; PPP,
663 pentose phosphate pathway; RNF, membrane-bound RNF complex; RSH/RS-SR,
664 reduced/oxidized disulfide; Sorb, sorbitol; TCA, tricarboxylic acid cycle; V, ATP synthase

665 complex; WLP, Wood Ljungdahl pathway; Xyl, xylitol. (B) Ecological distribution of
666 Candidatus “Zymogenia”-affiliated 16S rRNA sequences. The middle pie chart shows the
667 breakdown of hit sequences based on the classification of the environments from which they
668 were obtained (classification is based on the GOLD ecosystem classification scheme). Further
669 sub-classifications for each environment are shown as smaller pie charts.

References

1. Bikel S, Valdez-Lara A, Cornejo-Granados F. 2015. Combining metagenomics, metatranscriptomics and viromics to explore novel microbial interactions: towards a systems-level understanding of human microbiome. Comput Struct Biotechnol J 13:390-401.
2. Brown CT, Olm MR, Thomas BC, Banfield JF. 2016. Measurement of bacterial replication rates in microbial communities. Nat Biotechnol 34:1256-1263.
3. Rinke C, Schwientek P, Sczyrba A, Ivanova NN, Anderson IJ, Cheng JF, Darling A, Malfatti S, Swan BK, Gies EA, Dodsworth JA, Hedlund BP, Tsiamis G, Sievert SM, Liu WT, Eisen JA, Hallam SJ, Kyrpides NC, Stepanauskas R, Rubin EM, Hugenholtz P, Woyke T. 2013. Insights into the phylogeny and coding potential of microbial dark matter. Nature 499:431-7.
4. Wrighton KC, Thomas BC, Sharon I, Miller CS, Castelle CJ, VerBerkmoes NC, Wilkins MJ, Hettich RL, Lipton MS, Williams KH, Long PE, Banfield JF. 2012. Fermentation, hydrogen, and sulfur metabolism in multiple uncultivated bacterial phyla. Science 337:1661-5.
5. Anantharaman K, Brown CT, Hug LA, Sharon I, Castelle CJ, Probst AJ, Thomas BC, Singh A, Wilkins MJ, Karaoz U, Brodie EL, Williams KH, Hubbard SS, Banfield JF. 2016. Thousands of microbial genomes shed light on interconnected biogeochemical processes in an aquifer system. 7:13219.
6. Laura A Hug BJB, Karthik Anantharaman, Christopher T Brown, Alexander J Probst, Cindy J Castelle, Cristina N Butterfield, Alex W Hernsdorf, Yuki Amano, Kotaro Ise, Yohey Suzuki, Natasha Dudek, David A Relman, Kari M Finstad, Ronald Amundson, Brian C Thomas, Jillian F Banfield. 2016. A new view of the tree of life. Nature Microbiology:16048.
7. Parks DH, al. e. 2018. A standardized bacterial taxonomy based on genome phylogeny substantially revises the tree of life. Nature Biotechnol 36:996-1004.
8. Chaumeil PA, Mussig AJ, Hugenholtz P, Parks DH. 2019. GTDB-Tk: a toolkit to classify genomes with the Genome Taxonomy Database. Bioinformatics 36:1925-1927.
9. Quast C, Pruesse E, Yilmaz P, Gerken J, Schweer T, Yarza P, Peplies J, Glöckner FO. 2013. The SILVA ribosomal RNA gene database project: improved data processing and web-based tools. Nucl Acids Res 41:D590-D596. .
10. Hahn MW, Schmidt J, Koll U, Rohde M, Verbarg S, Pitt A, Nakai R, Naganuma T, Lang E. 2017. Silvanigrella aquatica gen. nov., sp. nov., isolated from a freshwater lake, description of Silvanigrellaceae fam. nov. and Silvanigrellales ord. nov., reclassification of the order Bdellovibrionales in the class Oligoflexia, reclassification of the families Bacteriovoracaceae and Halobacteriovoraceae in the new order Bacteriovoracales ord. nov., and reclassification of the family Pseudobacteriovoracaceae in the order Oligoflexales. Int J Syst Evoll Microbiol 67:2555-2568.
11. Waite DW, Chuvochina M, Pelikan C, Parks DH, Yilmaz P, Wagner M, Loy A, Naganuma T, Nakai R, Whitman WB, Hahn MW, Kuever J, Hugenholtz P. 2020. Proposal to reclassify the proteobacterial classes Deltaproteobacteria and Oligoflexia, and the phylum Thermodesulfobacteria into four phyla reflecting major functional capabilities. Int J Syst Evoll Microbiol 70:5972-6016.

12. Muyzer G, Stams AJM. 2008. The ecology and biotechnology of sulphate-reducing bacteria. Nature Rev Microbiol 6:441-454.
13. Kuever J. 2014. The Family Desulfobulbaceae. *In* Rosenberg E, DeLong EF, Loy S, Stackebrandt E, Thompson F (ed), The Prokaryotes: Deltaproteobacteria and Epsilonpoteobacteria. Springer-Verlag, Berlin Heidelberg
14. Greene AG. 2014. The Family Desulfuromonadaceae. *In* Rosenberg E, DeLong EF, Loy S, Stackebrandt E, Thompson F (ed), The Prokaryotes: Deltaproteobacteria and Epsilonpoteobacteria. Springer-Verlag, Berlin Heidelberg
15. Simon J, H.Kroneck PM. 2013. Microbial Sulfite Respiration. Adv Microbial Physiol 62:45-117.
16. Lovley DR, Giovannoni SJ, White DC, Champine JE, Phillips EJ, Gorby YA, Goodwin S. 1993. *Geobacter metallireducens* gen. nov. sp. nov., a microorganism capable of coupling the complete oxidation of organic compounds to the reduction of iron and other metals. Arch Microbiol 159:336-344.
17. Liu Y, Balkwill DL, Aldrich HC, Drake GR, Boone DR. 1999. Characterization of the anaerobic propionate-degrading syntrophs *Smithella propionica* gen. nov, sp. nov. and *Syntrophobacter wolinii*. Int J Syst Bacteriol 49:545-556.
18. Jackson BE, Bhupathiraju VK, Tanner RS, Woese CR, McInerney MJ. 1999. Syntrophus aciditrophicus sp. nov., a new anaerobic bacterium that degrades fatty acids and benzoate in syntrophic association with hydrogen-using microorganisms. Arch Microbiol 171:107-114.
19. Nayfach S, Roux S, Seshadri R, Udwary D, Varghese N, Schulz F, Wu D, Paez-Espino D, Chen IM, Huntemann M, Palaniappan K, Ladau J, Mukherjee S, Reddy TBK, Nielsen T, Kirton E, Faria JP, Edirisinghe JN, Henry CS, Jungbluth SP, Chivian D, Dehal P, Wood-Charlson EM, Arkin AP, Tringe SG, Visel A, Consortium IMD, Woyke T, Mouncey NJ, Ivanova NN, Kyrpides NC, Eloe-Fadrosh EA. 2020. A genomic catalog of Earth's microbiomes. Nat Biotechnol doi:10.1038/s41587-020-0718-6.
20. Elshahed MS, Senko JM, Najar FZ, Kenton SM, Roe BA, Dewers TA, Spear JR, Krumholz LR. 2003. Bacterial diversity and sulfur cycling in a mesophilic sulfide-rich spring. Appl Environ Microbiol 69:5609-5621.
21. Senko JM, Campbell BS, Henricksen JR, Elshahed MS, Dewers TA, Krumholz LR. 2004. Barite deposition mediated by photootrophic sulfide-oxidizing bacteria. Geochim Cosmochim Acta 68:773-780.
22. Buhring SI, Sievert SM, Jonkers HM, Ertefai T, Elshahed MS, Krumholz LR, Hinrichs K-U. 2011. Insights into chemotaxonomic composition and carbon cycling of phototrophic communities in an artesian sulfur-rich spring (Zodletone, Oklahoma, USA), a possible analog for ancient microbial mat systems. Geobiology 9:166-179.
23. Spain AM, Najar FZ, Krumholz LR, Elshahed MS. 2015. Comparative Metratranscriptomic analysis of a high-sulfide spring reveals insight into sulfur cycling pathways and unexpected aerobic metabolism. Peer J 33:e1259.
24. Li D, Liu C-M, Luo R, Sadakane K, Lam T-W. 2015. MEGAHIT: an ultra-fast single-node solution for large and complex metagenomics assembly via succinct de Bruijn graph Bioinformatics 31:1674-1676.
25. Kang DD, Li F, Kirton E, Thomas A, Egan R, An H, Wang Z. 2019. MetaBAT 2: an adaptive binning algorithm for robust and efficient genome reconstruction from metagenome assemblies. PeerJ 7:e7359-e7359.

26. Wu Y-W, Simmons BA, Singer SW. 2015. MaxBin 2.0: an automated binning algorithm to recover genomes from multiple metagenomic datasets. Bioinformatics 32:605-607.
27. Sieber CMK, Probst AJ, Sharrar A, Thomas BC, Hess M, Tringe SG, Banfield JF. 2018. Recovery of genomes from metagenomes via a dereplication, aggregation and scoring strategy. Nature Microbiology 3:836-843.
28. Parks DH, Rinke C, Chuvochina M, Chaumeil PA, Woodcroft BJ, Evans PN, Hugenholtz P, Tyson GW. 2018. Recovery of nearly 8,000 metagenome-assembled genomes substantially expands the tree of life. Nat Microbiol 3:253.
29. D.H. Parks MI, C.T. Skennerton, P. Hugenholtz, G.W. Tyson. 2015. CheckM: assessing the quality of microbial genomes recovered from isolates, single cells, and metagenomes. Genome Res 25:1043-1055.
30. Bowers RM, Kyrpides NC, Stepanauskas R, Harmon-Smith M, Doud D, Reddy TBK, Schulz F, Jarett J, Rivers AR, Eloe-Fadrosh EA, Tringe SG, Ivanova NN, Copeland A, Clum A, Becraft ED, Malmstrom RR, Birren B, Podar M, Bork P, Weinstock GM, Garrity GM, Dodsworth JA, Yooseph S, Sutton G, Glöckner FO, Gilbert JA, Nelson WC, Hallam SJ, Jungbluth SP, Ettema TJG, Tighe S, Konstantinidis KT, Liu WT, Baker BJ, Rattei T, Eisen JA, Hedlund B, McMahon KD, Fierer N, Knight R, Finn R, Cochrane G, Karsch-Mizrachi I, Tyson GW, Rinke C, Lapidus A, Meyer F, Yilmaz P, Parks DH, Eren AM, et al. 2017. Minimum information about a single amplified genome (MISAG) and a metagenome-assembled genome (MIMAG) of bacteria and archaea. Nat Biotechnol 35:725-731.
31. Lagesen K, Hallin P, Rødland EA, Staerfeldt H-H, .Rognes T, Ussery DW. 2007. RNAmmer: consistent and rapid annotation of ribosomal RNA genes. Nucleic Acids Res 35:3100-3108.
32. Chan PP, Lowe TM. 2019. tRNAscan-SE: Searching for tRNA genes in genomic sequences. Methods Mol Biol 1962:1-14.
33. Stamatakis A. 2014. RAxML version 8: a tool for phylogenetic analysis and post-analysis of large phylogenies. Bioinformatics 30:1312-1313.
34. Hyatt D, Chen G-L, Locascio PF, Land ML, Larimer FW, Hauser LJ. 2010. Prodigal: prokaryotic gene recognition and translation initiation site identification. BMC Bioinformatics 11:119.
35. Kanehisa M, Sato Y, Morishima K. 2016. BlastKOALA and GhostKOALA: KEGG Tools for functional characterization of genome and metagenome sequences. J Mol Biol 428:726-731.
36. Kanehisa M, Sato Y. 2020. KEGG Mapper for inferring cellular functions from protein sequences. Protein Sci 29:28-35.
37. Sievers F, Higgins DG. 2018. Clustal Omega for making accurate alignments of many protein sequences. Protein Sci 27:135-145.
38. Mistry J, Finn RD, Eddy SR, Bateman A, Punta M. 2013. Challenges in homology search: HMMER3 and convergent evolution of coiled-coil regions. Nucleic Acids Res 41:e121.
39. Price MN, Dehal PS, Arkin AP. 2010. FastTree 2 – approximately maximum-likelihood trees for large alignments. PLOS ONE 5:e9490.
40. Garber AI, Nealson KH, Okamoto A, McAllister SM, Chan CS, Barco RA, Merino N. 2020. FeGenie: A Comprehensive tool for the identification of iron genes and iron gene neighborhoods in genome and metagenome assemblies. Frontiers in Microbiology 11.

41. Søndergaard D, Pedersen CNS, Greening C. 2016. HydDB: A web tool for hydrogenase classification and analysis. Sci Rep 6:34212.
42. Orf GS, Gisriel C, Redding KE. 2018. Evolution of photosynthetic reaction centers: insights from the structure of the heliobacterial reaction center. Photosynthesis Research 138:11-37.
43. Tsuji J, Shaw N, Nagashima S, Venkiteswaran J, Schiff S, Hanada S, Tank M, Neufeld J. 2020. Anoxygenic phototrophic Chloroflexota member uses a Type I reaction center. bioRxiv doi:10.1101/2020.07.07.190934:2020.07.07.190934.
44. Sadekar S, Raymond J, Blankenship RE. 2006. Conservation of distantly related membrane proteins: photosynthetic reaction centers share a common structural core. Mol Biol Evol 23:2001-7.
45. Waterhouse A, Bertoni M, Bienert S, Studer G, Tauriello G, Gumienny R, Heer FT, de Beer TAP, Rempfer C, Bordoli L, Lepore R, Schwede T. 2018. SWISS-MODEL: homology modelling of protein structures and complexes. Nucleic Acids Res 46:W296-w303.
46. Chen I-MA, Chu K, Palaniappan K, Pillay M, Ratner A, Huang J, Huntemann M, Varghese N, White JR, Seshadri R, Smirnova T, Kirton E, Jungbluth SP, Woyke T, Eloe-Fadrosh EA, Ivanova NN, Kyrpides NC. 2019. IMG/M v.5.0: an integrated data management and comparative analysis system for microbial genomes and microbiomes. Nucl Acids Res 47:666-677.
47. Mukherjee S, Stamatis D, Bertsch J, Ovchinnikova G, Katta HY, Mojica A, Chen I-MA, Kyrpides NC, Reddy TBK. 2019. Genomes OnLine database (GOLD) v.7: updates and new features. Nucl Acids Res 47:D649-D659.
48. Letunic I, Bork P. 2016. Interactive tree of life (iTOL) v3: an online tool for the display and annotation of phylogenetic and other trees. Nucleic acids research 44:W242-W245.
49. Deng X, Dohmae N, Nealson KH, Hashimoto K, Okamoto A. 2018. Multi-heme cytochromes provide a pathway for survival in energy-limited environments. Sci Adv 4:eaao5682.
50. Mowat CG, Rothery E, Miles CS, McIver L, Doherty MK, Drewette K, Taylor P, Walkinshaw MD, Chapman SK, Reid GA. 2004. Octaheme tetrathionate reductase is a respiratory enzyme with novel heme ligation. Nat Struct Mol Biol 11:1023-4.
51. Hinojosa-Leon M, Dubourdieu M, Sanchez-Crispin JA, Chippaux M. 1986. Tetrathionate reductase of Salmonella thyphimurium: a molybdenum containing enzyme. Biochem Biophys Res Commun 136:577-81.
52. Dietrich W, Klimmek O. 2002. The function of methyl-menaquinone-6 and polysulfide reductase membrane anchor (PsrC) in polysulfide respiration of *Wolinella succinogenes*. Eur J Biochem 269:1086-95.
53. Ozawa K, Meikari T, Motohashi K, Yoshida M, Akutsu H. 2000. Evidence for the presence of an F-type ATP synthase involved in sulfate respiration in *Desulfovibrio vulgaris*. J Bacteriol 182:2200-2206.
54. Schuchmann K, Müller V. 2016. Energetics and application of heterotrophy in acetogenic bacteria. Appl Environ Microbiol 82:4056-4069.
55. Youssef NH, Farag IF, Rudy S, Mulliner A, Walker K, Caldwell F, Miller M, Hoff W, Elshahed M. 2019. The Wood–Ljungdahl pathway as a key component of metabolic versatility in candidate phylum Bipolaricaulota (Acetothermia, OP1). Environmental Microbiology Reports 11:538-547.

852 56. Müller V. 2003. Energy conservation in acetogenic bacteria. Appl Environ Microbiol
853 69:6345-53.
854 57. Taylor CD, Wolfe RS. 1974. Structure and methylation of coenzyme M
855 (HSCH2CH2SO3). J Biol Chem 249:4879-85.
856 58. Krum JG, Ensign SA. 2000. Heterologous expression of bacterial Epoxyalkane:
857 Coenzyme M transferase and inducible coenzyme M biosynthesis in *Xanthobacter* strain
858 Py2 and *Rhodococcus rhodochrous* B276. J Bacteriol 182:2629-2634.
859 59. Allen JR, Clark DD, Krum JG, Ensign SA. 1999. A role for coenzyme M (2-
860 mercaptoethanesulfonic acid) in a bacterial pathway of aliphatic epoxide carboxylation.
861 Proc Natl Acad Sci 96:8432-8437.
862 60. Coleman NV, Spain JC. 2003. Epoxyalkane:Coenzyme M transferase in the ethene and
863 vinyl chloride biodegradation pathways of *Mycobacterium* strain JS60. J Bacteriol
864 185:5536-5545.
865 61. Partovi SE, Mus F, Gutknecht AE, Martinez HA, Tripet BP, Lange BM, DuBois JL,
866 Peters JW. 2018. Coenzyme M biosynthesis in bacteria involves phosphate elimination
867 by a functionally distinct member of the aspartase/fumarase superfamily. J Biol Chem
868 293:5236-5246.
869 62. Graham DE, Graupner M, Xu H, White RH. 2001. Identification of coenzyme M
870 biosynthetic 2-phosphosulfolactate phosphatase. European Journal of Biochemistry
871 268:5176-5188.
872 63. Mendler K, Chen H, Parks DH, Lobb B, Hug LA, Doxey AC. 2019. AnnoTree:
873 visualization and exploration of a functionally annotated microbial tree of life. Nucleic
874 Acids Res 47:4442-4448.
875 64. Magot M, Ravot G, Campaignolle X, Ollivier B, Patel BK, Fardeau ML, Thomas P,
876 Crolet JL, Garcia JL. 1997. *Dethiosulfovibrio peptidovorans* gen. nov., sp. nov., a new
877 anaerobic, slightly halophilic, thiosulfate-reducing bacterium from corroding offshore oil
878 wells. Int J Syst Bacteriol 47:818-24.
879 65. Sorokin DY, Tourova TP, Mussmann M, Muyzer G. 2008. *Dethiobacter alkaliphilus* gen.
880 nov. sp. nov., and *Desulfurivibrio alkaliphilus* gen. nov. sp. nov.: two novel
881 representatives of reductive sulfur cycle from soda lakes. Extremophiles 12:431-9.
882 66. Hug LA, Co R. 2018. It takes a village: Microbial communities thrive through
883 interactions and metabolic handoffs. mSystems 3:e00152-e00157.
884 67. Canfield DE, Habicht KS, Thamdrup B. 2000. The Archean sulfur cycle and the early
885 history of atmospheric oxygen. Science 299:658-661.
886 68. Ranjan S, Todd ZR, Sutherland JD, Sasselov DD. 2018. Sulfidic anion concentrations on
887 early earth for surficial origins-of-Life chemistry. Astrobiology 18:1023-1041.
888 69. Fike DA, Bradley AS, Rose CV. 2015. Rethinking the anceint sulfur cycle. Annu Rev
889 Earth Planet Sci 43:593-622.
890 70. Hashimoto H, Uragami C, Cogdell RJ. 2016. Carotenoids and photosynthesis. Subcell
891 Biochem 79:111-39.
892 71. Du XJ, Wang XY, Dong X, Li P, Wang S. 2018. Characterization of the desiccation
893 tolerance of *Cronobacter sakazakii* strains. Front Microbiol 9:2867.
894 72. Krisko A, Radman M. 2013. Biology of extreme radiation resistance: the way of
895 *Deinococcus radiodurans*. Cold Spring Harb Perspect Biol 5: a012765.
896 73. Fiedor J, Sulikowska A, Orzechowska A, Fiedor L, Burda K. 2012. Antioxidant effects of
897 carotenoids in a model pigment-protein complex. Acta Biochim Pol 59:61-4.

74. Murphy CL, Dunfield PF, Sheremet A, Spear JR, Stepanauskas R, Woyke T, Elshahed MS, Youssef NH. 2020. Methylotrophy, alkane-degradation, and pigment production as defining features of the globally distributed yet-uncultured phylum Binatota. bioRxiv doi:10.1101/2020.09.14.296780:2020.09.14.296780.
75. Martin WF, Bryant DA, Beatty JT. 2018. A physiological perspective on the origin and evolution of photosynthesis. FEMS Microbiol Rev 42:205-231.
76. Nakamura T, Yamada KD, Tomii K, Katoh K. 2018. Parallelization of MAFFT for large-scale multiple sequence alignments. Bioinformatics 34:2490-2492.
77. Stamatakis A. 2014. RAxML version 8: a tool for phylogenetic analysis and post-analysis of large phylogenies. Bioinformatics 30:1312-3.
78. Fortunato CS, Larson B, Butterfield DA, Huber JA. 2018. Spatially distinct, temporally stable microbial populations mediate biogeochemical cycling at and below the seafloor in hydrothermal vent fluids. Environ Microbiol 20:769-784.
79. Dombrowski N, Teske AP, Baker BJ. 2018. Expansive microbial metabolic versatility and biodiversity in dynamic Guaymas Basin hydrothermal sediments. Nat Commun 9:4999.
80. Panwar P, Allen MA, Williams TJ, Hancock AM, Brazendale S, Bevington J, Roux S, Páez-Espino D, Nayfach S, Berg M, Schulz F, Chen IA, Huntemann M, Shapiro N, Kyrpides NC, Woyke T, Eloe-Fadrosh EA, Cavicchioli R. 2020. Influence of the polar light cycle on seasonal dynamics of an Antarctic lake microbial community. Microbiome 8:116.

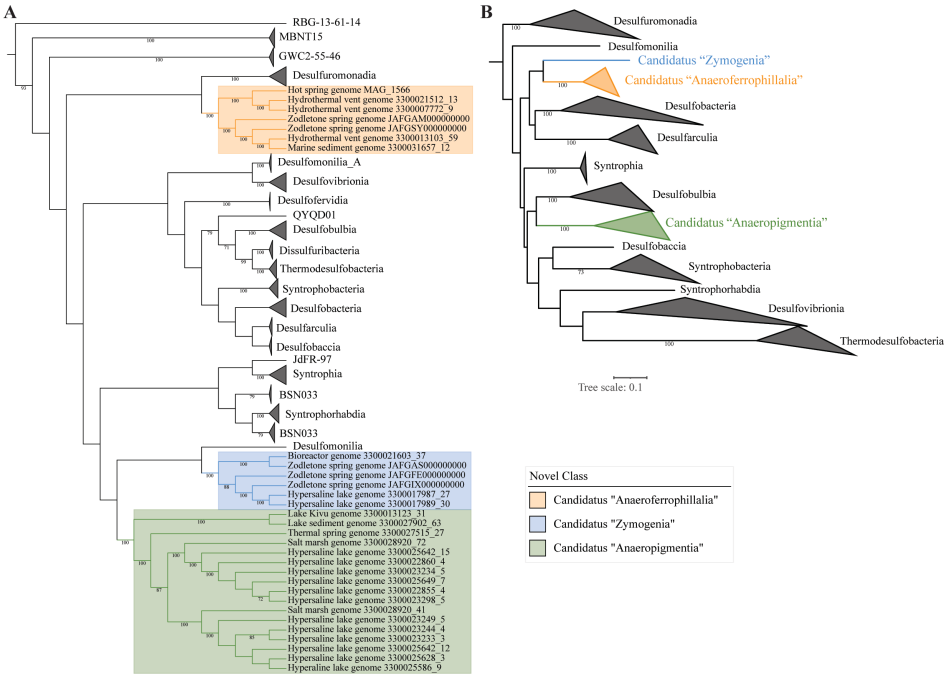

920

921

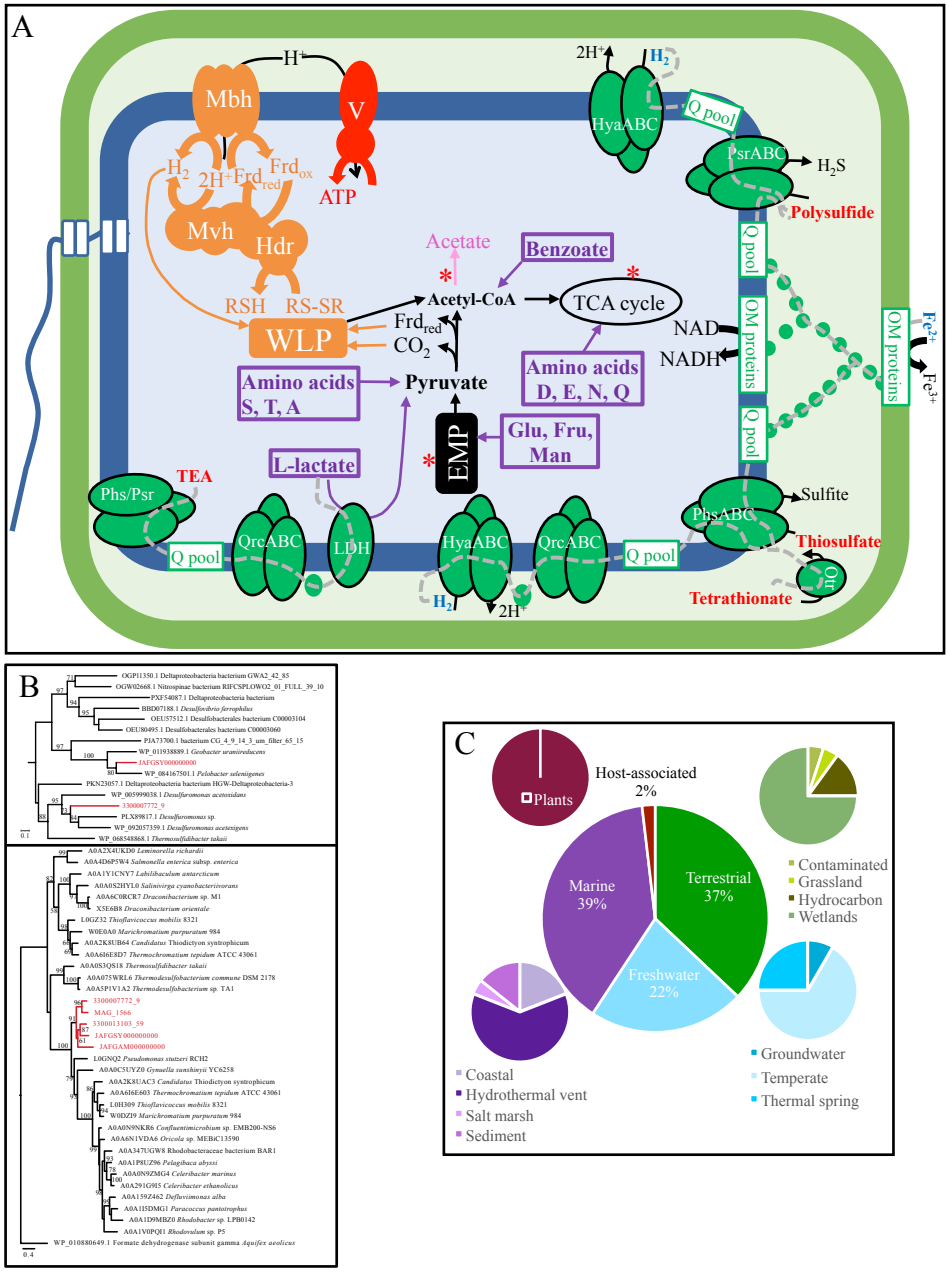

922

923 Figure 1

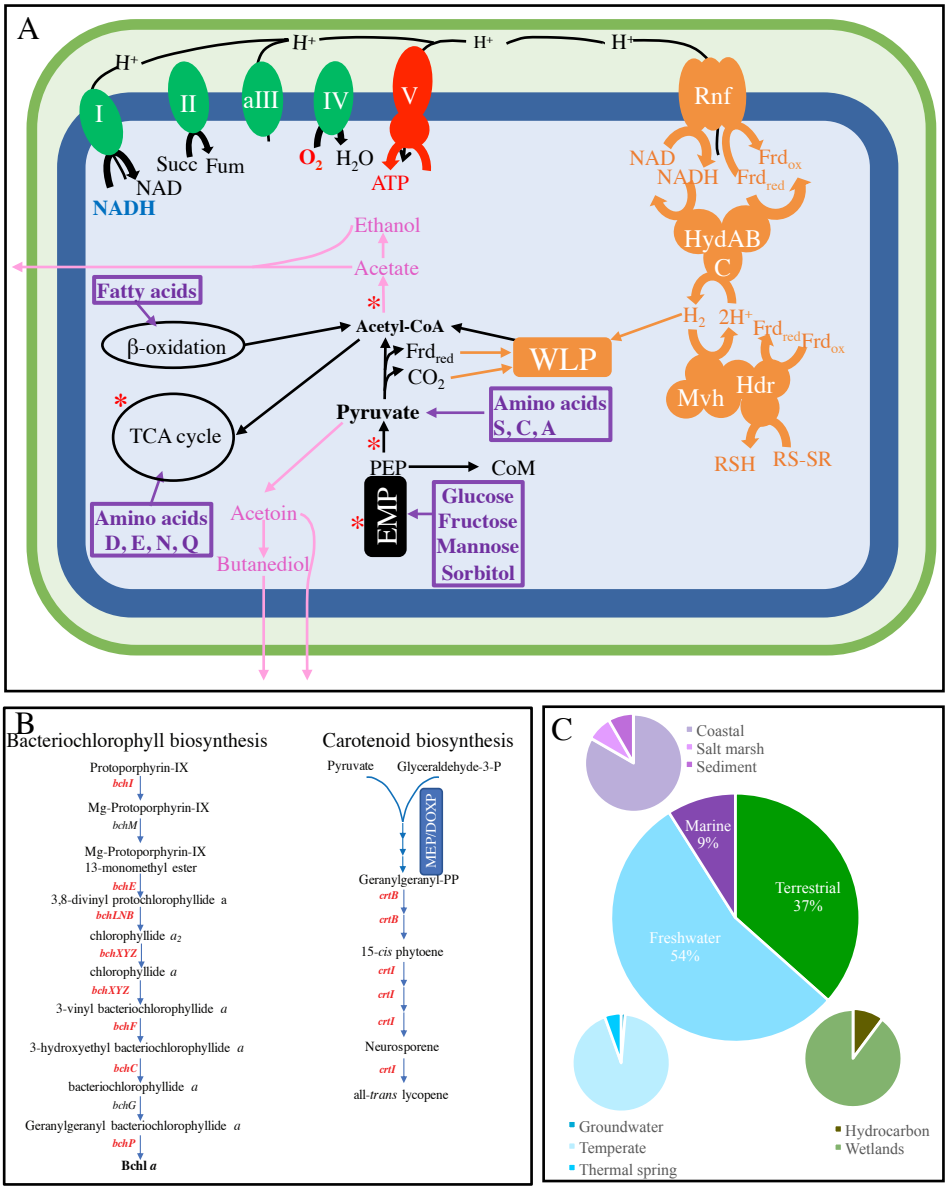

924

925 Figure 2

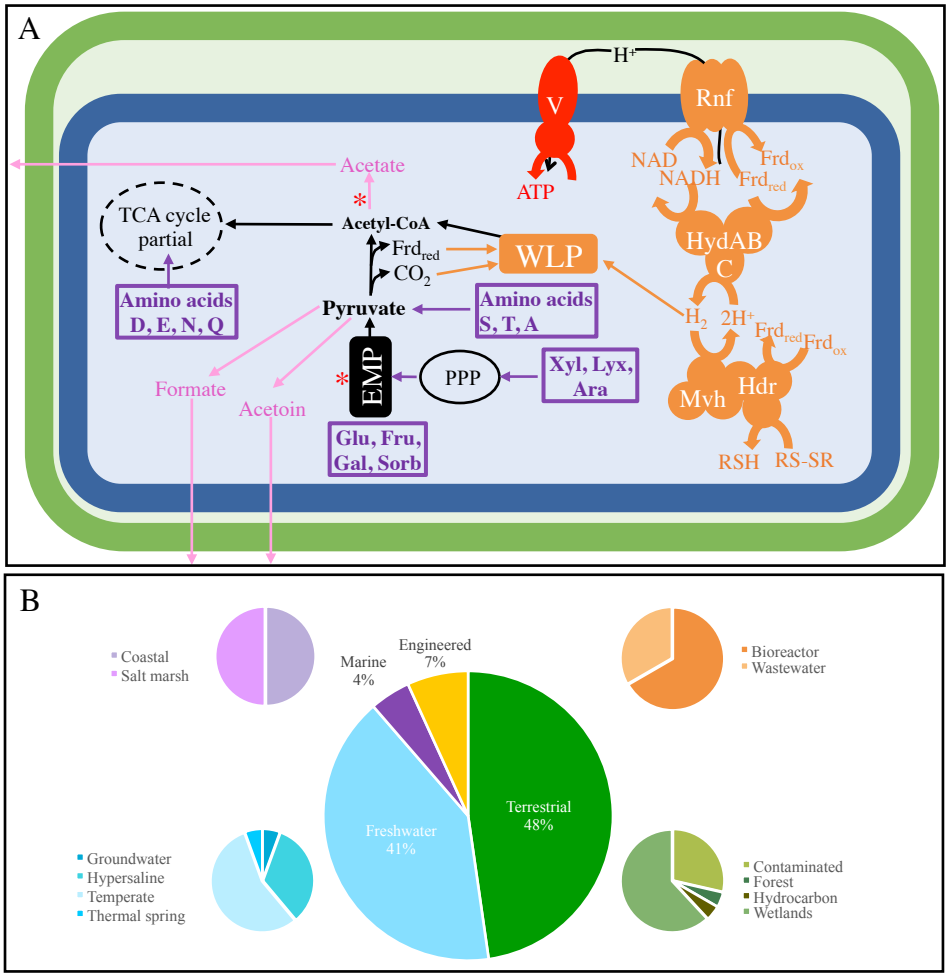

926
927 Figure 3

Table 1. General genomic features of the studied genomes.

Bin Name†	GenBank assembly accession number†	Assembly Size (Mbp)	Expected Genome Size (Mbp)	GC %	Number of Genes	Coding %	Ecosystem classification (level 1)	Ecosystem sub classification (level 2)	Site Geographical Location	References	
										NCBI BioProject ID	Citation
3300007772_9		1.62	2.44	48.18	1653	91.58	Marine	Hydrothermal vent	Axial Seamount	PRJEB22514	78
3300021512_13		1.54	2.77	47.98	1543	89.89	Marine	Hydrothermal vent	Guaymas Basin vent	PRJNA444987	
3300022547		**2.62**	**2.76**	**54.41**	**2438**	**88.24**	**Freshwater**	**Thermal spring**	**Wilbur Springs, CA**	PRJNA364781	
3300013103_59		1.56	2.91	53.95	1523	89.96	Marine	Hydrothermal vent	Guaymas Basin vent	PRJNA368391	79
3300031657_12		1.82	2.53	47.22	1685	85.98	Marine	Sediment	Southern Ocean, Antarctica	PRJNA518182	
Zgenome_940	JAFGSY01	2.7	2.74	53.55	2471	89.72	Freshwater	Sediment	Zodletone Spring, OK	PRJNA690107	This study
Zgenome_0214	JAFGAM01	2.68	3.44	63.31	2363	86.91	Freshwater	Sediment	Zodletone Spring, OK	PRJNA690107	This study
3300023233_3		4.81	5.07	41.66	4638	83.06	Freshwater	Hypersaline	Ace Lake, Antarctica	PRJNA467265	80
3300023244_4		3.96	4.39	41.42	3755	83.06	Freshwater	Hypersaline	Ace Lake, Antarctica	PRJNA467197	80
3300023249_5		4.15	4.49	41.9	3893	83.31	Freshwater	Hypersaline	Ace Lake, Antarctica	PRJNA467248	80
3300025586_9		3.77	4.56	42.11	3529	82.98	Freshwater	Hypersaline	Ace Lake, Antarctica	PRJNA375651	80
3300025628_3		4.04	4.64	41.98	3788	82.85	Freshwater	Hypersaline	Ace Lake, Antarctica	PRJNA367219	80
3300025642_12		3.83	4.7	42.16	3578	83.09	Freshwater	Hypersaline	Ace Lake, Antarctica	PRJNA367224	80
3300028920_41		3.47	4.6	50.24	3129	87.61	Marine	Salt marsh	Falmouth, MA	PRJNA518321	
3300022855_4		**3.31**	**3.4**	**48.79**	**2957**	**85.77**	**Freshwater**	**Hypersaline**	**Ace Lake, Antarctica**	**PRJNA467247**	**80**

3300023234_5		3.18	3.35	49.09	2914	85.94	Freshwater	Hypersaline	Ace Lake, Antarctica	PRJNA467206	80
3300023298_5		3.22	3.39	48.95	2899	85.99	Freshwater	Hypersaline	Ace Lake, Antarctica	PRJNA467209	80
3300025642_15		3.19	3.36	48.98	2962	86.37	Freshwater	Hypersaline	Ace Lake, Antarctica	PRJNA367224	80
3300025649_7		3.79	3.92	48.75	3447	85.81	Freshwater	Hypersaline	Ace Lake, Antarctica	PRJNA367218	80
3300028920_72		2.23	3.25	57.19	2212	87.31	Marine	Salt marsh	Falmouth, MA	PRJNA518321	
3300013123_31		3.2	4.73	50.1	3098	84.18	Freshwater	Temperate	Lake Kivu, Congo	PRJNA404433	
3300027902_63		1.26	2.41	50.99	1326	88.93	Freshwater	Sediment	University of Notre Dame, IN	PRJNA365732	
3300027515_27		2.72	3.34	50.49	2445	89.96	Freshwater	Thermal spring	Thermal spring, YNP	PRJNA367150	
3300017987_27		3.56	3.68	52.62	3284	85.75	Freshwater	Hypersaline	Salton Sea, CA	PRJNA444013	
3300017989_30		3.48	3.66	52.53	3203	85.76	Freshwater	Hypersaline	Salton Sea, CA	PRJNA444014	
Zgenome_24	**JAFGIX01**	**3.76**	**3.84**	**51.37**	**3350**	**84.54**	**Freshwater**	**Sediment**	**Zodletone Spring, OK**	**PRJNA690107**	This study
3300021603_37		2.2	3.54	58.54	2397	87.12	Engineered	Bioreactor	Toronto, ON	PRJNA501900	
Zgenome_0311	JAFGAS01	2.94	3.65	55.99	2730	86.46	Freshwater	Sediment	Zodletone Spring, OK	PRJNA690107	This study
Zgenome_1292	JAFGFE01	3.73	3.84	55.37	3398	87.75	Freshwater	Sediment	Zodletone Spring, OK	PRJNA690107	This study

†: Accession numbers here include the Metagenome Bin name (numbers starting with 33000; searchable at https://img.jgi.doe.gov/cgi-bin/mer/main.cgi?section=MetagenomeBinSearch&page=searchForm), and the NCBI assembly accession numbers for Zodletone MAGs.

Type strains are listed in **bold**.